Construction and Characterization of Cy3- or Cy5-Conjugated Hairpin Pyrrole/Imidazole Polyamides binding to DNA in the Nucleosome

Yong-Woon Han[*†,a,b], Tomoko Matsumoto[†a,c], Hiroaki Yokota[a], Yasuo Tsunaka[a,d], Gengo Kashiwazaki[e], Hironobu Morinaga[e], Kaori Hashiya[e], Toshikazu Bando[e], Hiroshi Sugiyama[*,a,b,e] and Yoshie Harada[*,a]

[a]Institute for Integrated Cell-Materials Science (iCeMS), Kyoto University, Yoshida Honmachi, Sakyo, Kyoto 606-8501, Japan,

[b]CREST, Japan Science and Technology Corporation (JST), Sanbancho, Chiyoda-ku, Tokyo 102-0075, Japan

[c]Department of Human Life Studies, Doshisha Women's College of Liberal of Arts, Teramachi Nishiiru, Imadegawa-dori, Kamigyo, Kyoto 602-0893, Japan,

[d]PREST, Japan Science and Technology Corporation (JST), Sanbancho, Chiyoda-ku, Tokyo 102-0075, Japan

[e]Department of Chemistry, Graduate School of Science, Kitashirakawa-oiwakecho, Kyoto University, Sakyo, Kyoto 606-8502,

[†]Equal contribution

han.yongwoon.4u@kyoto-u.ac.jp; hs@kuchem.kyoto-u.ac.jp; harada.yoshie.4r@kyoto-u.ac.jp

Abstract

Sequence-specific DNA-binding modules, *N*-methylpyrrole (Py)-*N*-methylimidazole-(Im) polyamides have been recently conjugated with fluorophores, and some of these conjugates could be used for detection of specific DNA sequences. In this study, we synthesized two Py-Im polyamides **1** and **2**, which interact with the 145-bp nucleosome positioning sequence 601. We conjugated the cyanine dyes Cy3 or Cy5 with **1** or **2**. In the absence of target DNA, the fluorescent conjugate of a Py-Im polyamide had lower fluorescence intensity compared with Cy3 or Cy5 alone. In the presence of either the target DNA or nucleosome, the fluorescence intensity of the conjugates increased. Furthermore, we observed a Förster resonance energy transfer between the Cy3-Py-Im polyamide and Cy5-Py-Im polyamide on the nucleosome. These results open up the possibilities that fluorescent conjugates of Py-Im polyamides can be used for characterization of the dynamic interactions within protein-DNA complexes.

Introduction

N-Methylpyrrole (Py)-*N*-methylimidazole-(Im) polyamides are small molecules that can recognize specific DNA sequences in the minor groove of B-form DNA with DNA recognition rules.[1,2] Py favors the T, A, and C bases, excluding G and Im favors G. Lone pair of N3 in Im forms a hydrogen bond with 2 amino hydrogen of guanine. Anti-parallel pairings of Im/Py and Py/Im bind to the G•C and C•G sequence in DNA, respectively. Anti-parallel pairing of Py/Py binds to A•T and T•A degenerately.[1,2] Aliphatic β-alanine (β) can be substituted for Py. Anti-parallel pairings of Py/β and β/Py bind to A•T and T•A degenerately, and anti-parallel pairings of Im/β and β/Im specify G•C and C•G, respectively.[3,4]

A Py-Im polyamide can be used as a synthetic sequence-specific DNA-binding module. Py-Im polyamides that can bind to a promoter region have been designed to inhibit gene expression,[5-9] and a conjugate of a Py-Im polyamide with a peptide or a small organic molecule can serve as a synthetic transcriptional activator.[10-13] Various types of alkylating moiety-conjugated Py-Im polyamides have also been developed as

sequence-specific DNA-alkylating agents, and their chemical and biological properties have been investigated.[14-20] In addition to these applications of Py-Im polyamides to gene expression and sequence-specific DNA alkylation, to date, many of fluorescent conjugates of Py-Im polyamides have been synthesized, and some of them can be used as effective sequence-specific fluorescent probes.[21-26] Thus, it is also possible that fluorescent conjugates of Py-Im polyamides could be used for characterization of dynamic interactions within protein-DNA complexes. At present, there are no data in the literature regarding the binding of this sort of conjugates to protein-DNA complexes. In this study, we investigated how fluorescent conjugates of Py-Im polyamides bind to DNA in a nucleosome.

The nucleosome is a basic unit of eukaryotic chromatin and consists of approximately 150 bp DNA wrapped in 1.7 superhelical turns around a histone octamer. The histone octamer consists of two copies each of four histone proteins, H2A, H2B, H3, and H4.[27] Genetic processes such as transcription, DNA replication, recombination and repair and chromatin segregation depend on changes of chromatin structures.[28-31] The histone chaperone and chromatin remodeler are the enzymes

involved in chromatin assembly/disassembly and in nucleosome movement, ejection or exchange, which are crucial for the abovemetioned genetic processes.[30]

In this work, we synthesized two Py-Im polyamides targeting a nucleosome positioning sequence 601.[32] We conjugated the two Py-Im polyamides with a cyanine dye, either Cy3 or Cy5, and used the conjugates Cy3-Py-Im polyamide and Cy5-Py-Im polyamide as a fluorescence donor-acceptor pair. We also investigated Förster resonance energy transfer (FRET) between the Cy3 conjugated and the Cy5 conjugated Py-Im polyamide on the nucleosome.

Experimental Section

General Methods

The following abbreviations are used in this article: Fmoc, fluorenylmethoxycarbonyl; DMSO, dimethylsulfoxide; DMF, dimethylformamide; DIEA, N,N-diisopropylethylamine; TFA, trifluoroacetic acid; Dp, 3-(dimethylamino)propylamine; EDTA, ethylenediaminetetraacetic acid; HEPES, 4-(2-hydroxyethyl)-1-piperazineethanesulfonic acid; β, β-alanine; γ, γ-aminobutyric acid; Py, N-methylpyrrole; Im, N-methylimidazole; PEG, polyethylene glycol.

Electrospray ionization time-of-flight mass spectrometry (ESI-TOFMS) was performed on BioTOF II (Bruker Daltonics) mass spectrometer to determine the molecular weight of Py-Im polyamides **1**, **2**, and **5**-**8**.

Polyamide Synthesis

Py-Im polyamides **1** and **2** were synthesized in a stepwise reaction using Fmoc solid-phase protocol as described previously.[33] The synthesis was performed on a

Pioneer Peptide Synthesizer, PSSM-8 (Shimazu, Japan) in a computer-assisted mode on a 100 μmol scale (270 mg of Fmoc-β-alanine Wang resin, 120 mmol/g). After the synthesis, Dp was mixed with the resin and the mixture was incubated for 4 hrs at 55 ºC on a shaker at 550 rpm to detach the Py-Im polyamides from the resin. Purification of Py-Im polyamides **1** and **2** was performed on High-performance liquid chromatography (HPLC) PU-2080 Plus series system (JASCO Inc., Japan) using a 10 mm × 150 mm Chemcopak Chemcobond 5-ODS-H reverse-phase column in 0.1% TFA in water with acetonitrile as an eluent at a flow rate of 3 mL/min, and linear-gradient elution with acetonitrile (20%—60% acetonitrille in water) lasting 20 min with detection at 254 nm. The collected fractions were analyzed using ESI-TOFMS.

Cy3- and Cy5-conjugated Py-Im polyamides

Fluorescent conjugates of Py-Im Polyamides **5-8** were synthesized using a coupling reaction between the Py-Im polyamide **1** or **2** and either Cy3 *N*-hydroxysuccinimidyl (NHS-) ester **3** or Cy5-NHS ester **4**. The coupling reactions were performed in DMF containing DIEA, which was used as a coupling agent.

Approximately 1.0 mg of **3** or **4** was dissolved in 45 μL of DMF and then Py-Im polyamide **1** or **2** (approximately 1.5 mg) was dissolved in the mixture. Next, 0.57 μL of DIEA was added to the reaction mixtures and the mixtures were incubated with shaking at 550 rpm for 2 h at room temperature. After the coupling reaction, 1 μL of the mixture was diluted with 9 μL DMF, and 1 μL of the diluted mixture was analyzed using the HPLC PU-2080 Plus series system with a 4.6 mm × 150 mm Chemcopak Chemcobond 5-ODS-H reverse-phase column in 0.1% TFA in water with acetonitrille as eluent at a flow rate of 1 mL/min, using linear-gradient elution with acetonitrile (0% to 100% in water) lasting 20 min with detection at 254 nm. We obtained fractions for two major peaks and the red (Cy3) or blue (Cy5) solution corresponding to the later peak was further investigated. Those fractions were analyzed using ESI-TOFMS, and we confirmed that the fluorophore (Cy3 or Cy5) was conjugated with the Py-Im polyamide. After that, purification of Py-Im polyamides **5**-**8** was performed on by HPLC using PU-2080 Plus series system employing a 10 mm × 150 mm Chemcopak Chemcobond 5-ODS-H reverse-phase column in 0.1% TFA in water with acetonitrile as an eluent at a flow rate of 3 mL/min, using linear-gradient elution with acetonitrile

(20%—60% in water) for 20 min with detection at 254 nm. The collected fractions were analyzed using ESI-TOFMS.

DNA preparation

Biotinylated DNA oligonucleotides, ODN1 and ODN2 (Fig. 1B) were used for the measurement of the DNA binding activities of the Py-Im polyamides by SPR assays.

Two other DNA oligos, ODN3 and ODN4, were used as primers in PCR for amplification of a 145-bp DNA fragment containing nucleosome positioning sequence 601 from the plasmid pGEM3Z-601.[32,34] The sequences of ODN3 and ODN4 are as follows: ODN3, 5′-AGATCTTCGCGAGAAGACGATATCAGAATCCCGGTGCCGAGG-3′, and ODN4, 5′-TCGCGACGTCTCAGATATCGATGTATATATCTGACAC-3′. As shown in Figure 2, the 145 bp amplicon was then inserted into T7 Blue Vector (Novagen). The ligated DNAs were introduced into the *E.coli* strain DH5α. We purified plasmid DNAs using Wizard Plus SV Minipreps DNA Purification System (Promega, USA) according to the vendor's manual and confirmed that the purified

plasmid DNA, pYT145-1, contained the 145-bp insert by 0.8% agarose gel electrophoresis. Next, pYT145-1 was digested with *Bbs*I and *Bsm*BI restriction endonucleases, and the resulting *Bbs*I-*Bsm*BI fragment containing the 145-bp DNA region of interest was inserted into *Bbs*I-digested dephosphorylated pYT145-1 (Fig. 2). The ligated DNA was introduced into DH5α, and after plasmid DNA purification, we checked the DNA using 0.8% agarose gel electrophoresis. Most of the purified plasmid DNA contained two copies of the 145-bp DNA region, and we used the plasmid, pYT145-2 to construct pYT145-4 (Fig. 2). The pYT145-2 was digested with *Bbs*I and *Bsm*BI and the *Bbs*I-*Bsm*BI fragment containing the 145-bp DNA region was inserted into *Bbs*I-digested dephosphorylated pYT145-2. The ligated DNAs were introduced into DH5α, and after plasmid DNA purification, we checked the DNA using 0.8% agarose gel electrophoresis. Most of the purified plasmid DNA contained four copies of the 145-bp DNA region, and we named this plasmid pYT145-4 (Fig. 2). After that, pYT145-4 was digested with *Bbs*I and *Bsm*BI and the fragment containing the 145-bp DNA of interest was inserted into *Bbs*I-digested dephosphorylated pYT145-4. The ligated DNA was introduced into DH5α, and after plasmid DNA purification, we

checked the DNA using 0.8% agarose gel electrophoresis. Most of the purified plasmid DNA contained eight copies of the 145-bp DNA region. Some of the purified plasmid DNA, however, contained more copies unexpectedly and, among them, we found pYT145-24, which contained 24 copies of the 145-bp DNA fragment. We used pYT145-24 for purification of the 145-bp DNA region as follow.

To obtain a large amount of pYT145-24, we introduced the plasmid into DH5α and one of the resultant colony was inoculated into 4 mL of Terrific broth (TB).[35] The culture was incubated for 4 hrs at 37 ºC with shaking. Next, equal amounts (0.5 mL) of the culture were transferred to eight conical flasks containing 100 mL TB and carbenicillin at 100 μg/mL. These flasks were incubated for approximately 16 h at 37 ºC with shaking. After that, pYT145-24 was purified using Nucleo Bond Xtra Maxi (Takara Bio, Japan) according to the vendor's manual.

For isolation of the 145-bp DNA fragment, the mixture (1 mL) containing 1 mg of pYT145-24 was mixed with *Eco*RV (600 units) and incubated at 37 ºC for approximately 16 h (Fig. 3A). Then, the 145-bp DNA was separated from the linearized vector DNA by means of PEG precipitation (Fig. 3A). We added 342 μL of

40% PEG4000 and 152 μL of 4M NaCl to the 1-mL mixture and the mixture was incubated on ice for 1 h. The linearized vector DNA was pelleted by centrifugation at 20,000 g and 4 ºC for 20 min. The 145-bp DNA in the supernatant was precipitated using a standard ethanol precipitation method, and the resulting DNA pellet was dissolved in 100 μL of HE buffer (10 mM HEPES, 1 mM EDTA, pH 8.0).

The earlier pellet from PEG precipitation (Fig. 3A) was dissolved in 1 mL of HE buffer and checked using 1.2% agarose gel electrophoresis. Because the 145-bp DNA was still present in that pellet, 342 μL of 40% PEG4000 and 152 μL of 4M NaCl were added to the 1-mL mixture and the 145-bp DNA was separated from the linearized vector DNA as described above (Fig. 3A). The 145-bp DNA in the supernatant was collected using ethanol precipitation and the pellet was dissolved in 100 μL of HE buffer. We confirmed that only trace amounts of the 145-bp DNA were present in the pellet from the second PEG precipitation (Fig. 3A). The yield of the 145-bp DNA was approximately 0.32 mg.

Mononucleosome preparation

A histone octamer was prepared as described previously.[34] Mononucleosomes were assembled using a salt dialysis method from the histone octamer and the-145 bp DNA fragment as follows. The histone octamer and the 145-bp DNA were mixed in 300 μL of Buffer A (20 mM HEPES, 0.1 mM EDTA, pH 7.5) containing 2 M NaCl. The final concentration of the histone octamer and DNA was 0.5 μM. The mixture was transferred to the dialysis tube, Oscillatory Cup MWCO 8000 (Cosmo Bio Co., Ltd., Japan), and the dialysis against 500 mL of the Buffer A containing 2 M NaCl was started at 4 ºC under constant stirring. After 2 h, the buffer was changed to 500 mL of fresh Buffer A containing 1.5 M NaCl and the dialysis was continued for approximately 16 h additionally. Several more stages of dialysis, with changes to a fresh buffer, were performed as shown in Figure 3B. After the dialysis, the mixture was checked using 5 % polyacrylamide gel electrophoresis and we confirmed that >95% of DNA formed complexes with the histone octamer (Fig. 3C). The concentration of the nucleosome was determined spectrophotometrically using $\varepsilon_{260} = 1.88 \times 10^6$ cm^{-1} M^{-1}.

Surface Plasmon Resonance (SPR) Assay

All SPR experiments were performed on a BIACORE X instrument at 25 ºC as described previously.[33,36-38] The sequences of biotinylated hairpin DNAs containing target sequences are described above. The hairpin DNAs were immobilized on a streptavidin-coated SA sensor chip at a flow rate of 20 μL/min to obtain the required immobilization level (up to approximately 1400 resonance units (RU) rise). The experiments were performed using HBS-EP (10 mM HEPES, 150 mM NaCl, 3 mM EDTA, and 0.005% Surfactant P20) buffer with 0.1% DMSO at 25 ºC, pH 7.4. A series of sample solutions were prepared in HBS-EP buffer with 0.1% DMSO and injected at a flow rate of 20 μL/min. To measure association and dissociation rate constants (K_D, k_a and k_d), data processing was performed with an appropriate fitting model using the BIAevaluation 4.1 program. The sensorgrams of all data were fitted using the 1:1 binding model with mass transfer. The values of K_D k_a and k_d for all data are summarized in Table 1.

Steady state fluorescence spectroscopy experiments

All steady-state fluorescence spectra measurements were made with a

spectrofluorometer FP-6500 (JASCO Inc., Japan), equipped with a Xenon 150-W lamp. Excitation and emission wavelengths are indicated in the figure legend and all data were collected at 25 ºC.

Results and Discussion

Synthesis of the conjugates of Py-Im polyamides with Cy3 or Cy5

As described in the Experimental Section, the 145-bp DNA of nucleosome positioning sequence 601 was used for preparation of the nucleosome. To characterize the binding of Py-Im polyamides to the nucleosome, we chose two DNA sites, TAAGC and ACGTGT (Fig. 4). Without a histone octamer, the distance between the two DNA sites was 75 bp, which corresponded to approximately 25 nm. In contrast, this distance within the nucleosome as shown in Figure 4A, was approximately 3 nm. Consequently, in this study, we synthesized two Py-Im Polyamides **1** and **2** (Fig. 1A), which contain two β-alanine residues at the N-terminus. We synthesized several Py-Im polyamides with this kind of N-terminus and demonstrated that β-Dp linker at the C-terminus had a slight steric preference for A•T or T•A over G•C or C•G.[37] Accordingly, the target DNA sequences of **1** and **2** were set as 5′-WWWGC-3′ and 5′-WCGWGW-3′, respectively (Fig. 4).

After the synthesis of **1** and **2**, we conjugated either Cy3 or Cy5 to the Py-Im

polyamides using Cy3-NHS ester **3** or Cy5-NHS ester **4** and obtained **5**-**8**. As shown in Figure 1A, **5** and **6** are Cy3- and Cy5-conjugated Py-Im polyamide **1**, respectively, whereas **7** and **8** are Cy3- and Cy5-conjugated Py-Im polyamide **2**. We confirmed that the purity of each conjugate, **5**-**8**, was >95 %, according to analytical HPLC and ESI-TOFMS.

SPR assay

To characterize the DNA binding affinity of **1**, **2** and **5**-**8**, the SPR experiments were performed as described in the Experimental Section, and the respective dissociation equilibrium constant (K_D), association rate constant (k_a), and dissociation rate constant (k_d) against the target DNAs were measured. As shown in Figure 5, the SPR sensorgrams were obtained and the kinetic binding parameters K_D, k_a and k_d were determined (Table 1). The K_D, k_a and k_d of **1** against ODN1 were 1.0×10^{-9} M, 8.3×10^6, $M^{-1}s^{-1}$, and 8.7×10^{-3} s^{-1}, respectively. In the case of **2**, the K_D, k_a and k_d were 1.0×10^{-9} M, 8.3×10^6, $M^{-1}s^{-1}$, and 8.7×10^{-3} s^{-1}, respectively, and comparable to those of **1**. We have measured the K_D, k_a and k_d of β-β-ImPyPyPy-γ-PyPyImPy-β-Dp against

ODN1[37] and compared with these data, the k_a and k_d of **1** were improved by 16 and 1.5-fold, respectively. These results suggest that the substitutions of β for Py improved the association rate constant but not the dissociation rate constant. We are now planning to synthesize a Py-Im polyamide with a single replacement of Py with β and to measure the binding kinetics. These studies will allow us to characterize in more detail the effect of this substitution on Py-Im polyamides targeting 5′-WWWGC-3′.

The K_Ds of **5** and **6** with ODN1 were 3.5×10^{-7} M and 6.4×10^{-8} M, respectively, which were decreased by 350 and 64-fold, respectively, compared to **1** (Table 1). In the case of **7** and **8**, their K_Ds with ODN2 were 3.1×10^{-7} M and 5.1×10^{-7} M, respectively, which were decreased by 530 and 860-fold, respectively (Table 1), compared to **2** (Table 1). The k_as and k_ds of **5-8** were diminished by 4.3- to 75-fold, compared to **1** or **2**. These data suggest that conjugation of Cy3 or Cy5 to the N-terminus of Py-Im polyamide probably weakens the binding of the Py-Im polyamide to its target DNA and lowers the stability of the Py-Im polyamide–DNA complex.

As reported previously, the K_D of a pyrene-conjugated Py-Im polyamide with its

target DNA is 8.3×10^{-7} M,[24] which is comparable with K_Ds of **5**-**8**; emission intensity of the pyrene-conjugated Py-Im polyamide increased in the presence of the target DNA. Therefore, in this study, we decided to measure the emission spectra of **5**-**8** as described below.

Binding of Cy3- or Cy5-conjugated Py-Im polyamides to DNA increases their fluorescence intensity

The DNA-binding processes of conjugates **5**-**8** were characterized using emission spectroscopy (Fig. 6). As reported previously, many fluorophore-conjugated Py-Im polyamides undergo a decrease of fluorescence intensity relative to the control fluorescence in the absence of their target DNA.[21-24] Thus, we also measured emission spectra of **3**-**8** in the absence of the target DNA. As shown in Figures 6A and B, in the absence of DNA, a fluorophore conjugated with a Py-Im polyamide shows a decrease in fluorescence intensity relative to the fluorophore alone. Compared with **3**, the fluorescence intensities of **5** and **7** decreased by 3.1- and 5.1-fold, respectively (Fig. 6A). The peak of emission spectrum from **3** was 562 nm, whereas peaks for both **5** and **7**

were 564 nm (Fig. 6A). In the case of Cy5-conjugated Py-Im polyamides (Fig. 6B), the fluorescence intensities of **6** and **8** decreased by 7.8- and 11-fold, respectively, compared with **4**. The peaks of emission spectra for **6** and **8** were 664 and 668 nm, respectively, whereas the peak for **4** was 662 nm (Fig. 6B).

Next, we obtained the spectrum for each conjugate **5**-**8** in the presence of the target DNA (Fig. 6C-F). At 50 nM of the DNA, the fluorescence intensities of **5**-**8** increased by 3.9-, 1.3-, 5.8- and 1.6-fold, respectively, compared with those without the DNA. At 200 nM of the DNA, the fluorescence intensities of **5**-**8** increased by 4.8-, 1.5-, 6.9- and 1.9-fold, respectively, compared with those without the DNA. From these data, the K_D of **5**-**8** against the target DNA were determined at 50–500 nM, and these constants are mostly consistent with the SPR data described above.

In the case of Cy3-conjugated Py-Im polyamides **5** and **7**, their fluorescence intensities increased significantly as a result of addition of their target DNA. In contrast, the fluorescence intensities of Cy5-conjugated Py-Im polyamides **6** and **8** increased insignificantly after the addition of their target DNA. The peaks of emission spectra for the Py-Im polyamides in the presence of the target DNA were similar to

those in the absence of the target DNA (Fig. 6C-F). These results suggest that Cy3- or Cy5-conjugated Py-Im polyamides could be useful as a fluorescent probe for detection of specific DNA sequences.

The Förster resonance energy transfer between the Cy3-Py-Im polyamide and Cy5-Py-Im polyamide on the nucleosome

As shown in Figure 4, the distance between the two target sequence sites in the 145-bp DNA is approximately 25 nm. But this distance decreased to approximately 3 nm when the DNA formed a nucleosome with the histone octamer (Fig. 4). Accordingly, we measured the emission spectrum of the mixture containing **5** and **8** with either DNA or nucleosome (Fig. 7) to demonstrate whether FRET occurs between **5** and **8** on the nucleosome. In the presence of the naked 145-bp DNA, the fluorescence intensity of the mixture containing **5** and **8** decreased slightly by 5% (between 550 nm and 620 nm), compared with the mixture containing only **5** and naked DNA (Fig. 7A). On the other hand, in the presence of the nucleosome, the fluorescence intensity of the mixture containing **5** and **8** decreased significantly by 28%

(between 550 nm and 620 nm), compared with the mixture containing only **5** and the nucleosome (Fig. 7B). These results suggest that emitted fluorescence by Cy3 in **5** was absorbed by Cy5 in **8** on the same nucleosome because the distance between the Cy3 and Cy5 moieties was approximately 3 nm, which is shorter than the Förster distance.[39] After that, we determined the emission spectra for **8** in the mixture containing **5**, **8**, and the nucleosome in order to demonstrate whether the fluorescence intensity of Cy5 in **8** increased as a result of the energy transfer from Cy3 in **5** on the same nucleosome. To determine the emission spectrum of **8**, the emission spectrum of **5** in the mixture containing **5**, **8**, and the nucleosome was subtracted from the emission spectrum of the mixturee. Because the fluorescence intensity between 550 nm and 620 nm of the mixture containing **5** and **8** decreased by 28%, compared with that containing **5**, the decrease by 28% from the emission spectrum of the mixture containing **5** was defined as the spillover from **5** in the mixture containing **5**, **8**, and the nucleosome. As shown in Figure 7C, the emission spectra from **5** in the mixture containing **5** and the spillover were almost identical between 550 nm and 620 nm. The calculated emission spectrum from **8** in the mixture containing **5**, **8**, and the nucleosome was determined by

subtracting the spillover from the emission spectrum of the mixture containing **5**, **8**, and the nucleosome (Fig. 7C and D). As shown in Figure 7D, the fluorescence intensity of **8** increased in the presence of the nucleosome, and furthermore, in the presence of both **5** and the nuclesome, the fluorescence intensity of **8** increased synergistically.

In the case of **7** and **6**, the fluorescence intensity of the mixture containing **7** and **6** decreased slightly by 5% (between 550 nm and 620 nm), compared with the mixture containing **7** in the presence of the naked 145-bp DNA (Fig. 8A). In contrast, in the presence of the nucleosome, the fluorescence intensity of the mixture containing **7** and **6** decreased significantly by 22% (between 550 nm and 620 nm), compared with that containing **7** (Fig. 8B). We also calculated the spillover from **7** in the mixture containing **7**, **6**, and the nucleosome (Fig. 8C) and determined the emission spectrum of **6** in the mixture containing **7**, **6**, and the nucleosome. Our data show that the fluorescence intensity of **6** was increased by the presence of **7** and the nucleosome (Fig. 8D) and FRET was observed between **7** and **6** on the nucleosome.

Previously, using a fluorescently labeled oligonucleotide, DNA fragments containing the nucleosome positioning sequence 601 have been constructed.[40-43] After

that, fluorescently labeled nucleosomes were constructed by mixing with the labeled DNA and the histone octamer[40-43] and the properties of ATP-dependent chromatin assembly and remodeling factor (ACF) were studied by means of FRET measurements of the fluorescently labeled nucleosomes.[40,41] In the present work, using **5** and **8** or **7** and **6** as a FRET donor-acceptor pair, FRET was observed between **5** and **8** and, separately, between **7** and **6** on the nucleosome, but not on the target DNA. These results suggest that it is possible to use a fluorescent conjugate of a Py-Im polyamide for characterization of enzymes, such as the histone chaperone or chromatin remodeler. We are now planning to prepare some chromatin remodelers for characterization using either spectroscopy or single-molecule fluorescence imaging techniques. If fluorophore conjugates of Py-Im polyamides can be successfully used for characterization of the histone chaperone or chromatin remodelers, then this kind of conjugate may also be applied to characterization of longer DNA-protein complexes such as those involved in DNA-looping. DNA-looping is performed by a protein-DNA complex consisting of multiple proteins that simultaneously bind to two DNA sites that are tens to thousands of base pairs apart.[44,45] DNA-looping that is

mediated by transcription factors or repressors regulates gene expression.[44,45] Site-specific DNA recombination by transposons such as bacteriophage Mu and retroviruses such as HIV-1 as well as V(D)J recombination also involves DNA-looping.[46-49] Fluorescent conjugates of the Py-Im polyamides that bind specifically to the DNA-sites that participate in the DNA-looping process will allow us to characterize these dynamic and complicated protein-DNA complexes.

Another application of fluorescent conjugates of Py-Im polyamides is the studies of DNA-based photonic wires.[50-53] W. Su et al. prepared 21-, 55- or 80-bp DNA fragments containing two fluorophores, Pacific Blue at one end and Cy3 at the other, as well as an oxazole yellow-conjugated Py-Im polyamide that binds to the internal regions of these DNAs. By measuring emission spectra of a mixture of the DNA and the Py-Im polyamide, they demonstrated that the oxazole yellow conjugate mediated the energy transfer from the Pacific Blue moiety to Cy3.[53] Similarly, in the present study, we observed FRET between a Cy3-conjugated and a Cy5-conjugated Py-Im polyamide on the same nucleosome. Thus, if protein-DNA complexes whose association and dissociation processes can be regulated become available, in the future, this will help us

to construct complicated controllable DNA-based photonic wires.

Conclusion

In this work, we synthesized Cy3- and Cy5-conjugated hairpin Py-Im polyamides targeting the 145-bp DNA containing nucleosome positioning sequence 601. In the presence of the nucleosome, strong fluorescence emission was observed from the Cy3 conjugate. Furthermore, we observed FRET between the Cy3-conjugated Py-Im polyamide **5** and Cy5-conjugated Py-Im polyamide **8** on the nucleosome. The same was true of **7** and **6**. These results suggest that fluorophore-conjugated Py-Im polyamides can be used for studies of protein-DNA complexes.

AUTHOR INFORMATION

Corresponding Authors.

han.yongwoon.4u@kyoto-u.ac.jp (Y.-W.H), hs@kuchem.kyoto-u.ac.jp (H.S), harada.yoshie.4r@kyoto-u.ac.jp (Y.H)

Acknowledgements

This work was supported by a Grant-in-Aid for Young Scientists (B) from the Ministry of Education, Culture, Sports, Science, and Technology, an iCeMS Exploratory Grants for Junior Investigators, an iCeMS-JSPS Overseas Visit Program for Young Researchers (Y.-W.H), Core Research for Evolutional Science and Technology (CREST) of the Japan Science and Technology Agency (Y.-W.H and H.S) and Funding Program for Next Generation World-Leading Researchers (Y.H). We thank Prof. K. Morikawa for valuable comments.

Notes and references

(1) P. B. Dervan, B. S. Edelson, *Curr. Opin. Struct. Biol.* **2003**, *13*, 284.

(2) P. B. Dervan, A. T. Poulin-Kerstien, E. J. Fechter, B. S. Edelson, *Topics in Current Chemistry* **2005**, *253*, 1.

(3) J. M. Turner, S. E. Swalley, E. E. Baird, P. B. Dervan, *J. Am. Chem. Soc.* **1998**, *120*, 6219.

(4) C. C. Wang, U. Ellervik, P. B. Dervan, *Bioorg. Med. Chem.* **2001**, *9*, 653.

(5) J. M. Gottesfeld, J. M.; Turner, P. B. Dervan, *Gene Expr.* **2000**, *9*, 77.

(6) E. J. Fechter, P. B. Dervan, *J. Am. Chem. Soc.* **2003**, *125*, 8476.

(7) M. S. Murty, H. Sugiyama, *Biol. Pharm. Bull.* **2004**, *27*, 468.

(8) N. G. Nickols, P. B. Dervan, *Proc. Natl. Acad. Sci. USA* **2007**, *104*, 10418.

(9) D. M. Chenoweth, D. A. Harki, J. W. Phillips, C. Dose, P. B. Dervan, *J. Am. Chem. Soc.* **2009**, *131*, 7182.

(10) A. K. Mapp, A. Z. Ansari, M. Ptashne, P. B. Dervan, *Proc. Natl. Acad. Sci. USA* **2000**, *97*, 3930.

(11) A. Z. Ansari, A. K. Mapp, D. H. Nguyen, P. B. Dervan, M. Ptashne, *Chemistry & Biology* **2001**, *8*, 583.

(12) P. S. Arora, A. Z. Ansari, T. P. Best, M. Ptashne, P. B. Dervan, *J. Am. Chem. Soc.* **2002**, *124*, 13067.

(13) Y. Kwon, H. D. Arndt, Q. Mao, Y. Choi, Y. Kawazoe, P. B. Dervan, M. Uesugi, *J. Am. Chem. Soc.* **2004**, *126*, 15940.

(14) T. Bando, H. Sugiyama, *Accounts of Chemical Research* **2006**, *39*, 935.

(15) T. Bando, S. Sasaki, M. Minoshima, C. Dohno, K. Shinohara, A. Narita, H. Sugiyama, *Bioconjug. Chem.* **2006**, *17*, 715.

(16) S. Sasaki, T. Bando, M. Minoshima, T. Shimizu, K.

Shinohara, T. Takaoka, H. Sugiyama, *J. Am. Chem. Soc.* **2006**, *128*, 12162.

(17) M. Minoshima, T. Bando, S. Sasaki, K. Shinohara, T. Shimizu, J. Fujimoto, H. Sugiyama, *J. Am. Chem. Soc.* **2007**, *129*, 5384.

(18) G. Kashiwazaki, T. Bando, K. Shinohara, M. Minoshima, H. Kumamoto, S. Nishijima, H. Sugiyama, *Bioorg. Med. Chem.* **2010**, *18*, 2887.

(19) M. Minoshima, T. Bando, K. Shinohara, G. Kashiwazaki, S. Nishijima, H. Sugiyama, *Bioorg. Med. Chem.* **2010**, *18*, 1236.

(20) S. Park, T. Bando, K. Shinohara, S. Nishijima, H. Sugiyama, *Bioconjug. Chem.* **2011**, *22*, 120.

(21) V. C. Rucker, S. Foister, C. Melander, P. B. Dervan, *J. Am. Chem. Soc.* **2003**, *125*, 1195.

(22) E. J. Fechter, B. Olenyuk, P. B. Dervan, *J. Am. Chem. Soc.* **2005**, *127*, 16685.

(23) T. Bando, J. Fujimoto, M. Minoshima, K. Shinohara, S. Sasaki, G. Kashiwazaki, M. Mizumura, H. Sugiyama, *Bioorg. Med. Chem.* **2007**, *15*, 6937.

(24) J. Fujimoto, T. Bando, M. Minoshima, G. Kashiwazaki, S. Nishijima, K. Shinohara, H. Sugiyama, *Bioorg. Med. Chem.* **2008**, *16*, 9741.

(25) T. Vaijayanthi, T. Bando, G. N. Pandian, H. Sugiyama, *Chembiochem* **2012**, *13*, 2170.

(26) T. Vaijayanthi, T. Bando, K. Hashiya, G. N. Pandian, H. Sugiyama, *Bioorg. Med. Chem.* **2013**, *21*, 852.

(27) K. Luger, *Curr. Opin. Genet. Dev.* **2003**, *13*, 127.

(28) K. Ohta, A. Nicolas, M. Furuse, A. Nabetani, H. Ogawa, T. Shibata, *Proc. Natl. Acad. Sci. USA* **1998**, *95*, 646.

(29) P. B. Becker, W. Horz, *Annu. Rev. Biochem.* **2002**, *71*, 247.

(30) C. R. Clapier, B. R. Cairns, *Annu. Rev. Biochem.* **2009**, *78*, 273.

(31) B. D. Price, A. D. D'Andrea, *Cell* **2013**, *152*, 1344.

(32) P. T. Lowary, J. Widom, *J. Mol. Biol.* **1998**, *276*, 19.

(33) M. Minoshima, T. Bando, S. Sasaki, J. Fujimoto, H. Sugiyama, *Nucleic Acids Res.* **2008**, *36*, 2889.

(34) Y. Tsunaka, J. Toga, H. Yamaguchi, S. Tate, S. Hirose, K.

Morikawa, K. *J. Biol. Chem.* **2009**, *284*, 24610.

(35) P. N. Dyer, R. S. Edayathumangalam, C. L. White, Y. Bao, S. Chakravarthy, U. M. Muthurajan, K. Luger, K. *Methods Enzymol.* **2004**, *375*, 23.

(36) W. Zhang, T. Bando, H. Sugiyama, *J. Am. Chem. Soc.* **2006**, *128*, 8766.

(37) Y. W. Han, T. Matsumoto, H. Yokota, G. Kashiwazaki, H. Morinaga, K. Hashiya, T. Bando, Y. Harada, H. Sugiyama, H. *Nucleic Acids Res.* **2012**, *40*, 11510.

(38) Y. W. Han, G. Kashiwazaki, H. Morinaga, T. Matsumoto, K. Hashiya, T. Bando, Y. Harada, H. Sugiyama, *Bioorg. Med. Chem.* **2013,** *21*, 5436.

(39) P. Wu, L. Brand, *Anal. Biochem.* **1994**, *218*, 1.

(40) J. G. Yang, T. S. Madrid, E. Sevastopoulos, G. J. Narlikar, *Nat. Struct. Mol. Biol.* **2006**, *13*, 1078.

(41) T. R. Blosser, J. G. Yang, M. D. Stone, G. J. Narlikar, X. Zhuang, *Nature* **2009**, *462*, 1022.

(42) M. G. Poirier, E. Oh, H. S. Tims, J. Widom, *Nat. Struct. Mol. Biol.* **2009**, *16*, 938.

(43) M. R. Duan, M. J. Smerdon, *J. Biol. Chem.* **2010**, *285*, 26295.

(44) K. S. Matthews, *Microbiol. Rev.* **1992**, *56*, 123.

(45) R. Schleif, *Annu. Rev. Biochem.* **1992**, *61*, 199.

(46) R. Craigie, K. Mizuuchi, *Cell* **1986**, *45*, 793.

(47) K. Adzuma, K. Mizuuchi, *Cell* **1989**, *57*, 41.

(48) D. C. van Gent, K. Mizuuchi, M. Gellert, *Science* **1996**, *271*, 1592.

(49) A. Engelman, K. Mizuuchi, R. Craigie, *Cell* **1991**, *67*, 1211.

(50) M. Heilemann, R. Kasper, P. Tinnefeld, M. Sauer, *J. Am. Chem. Soc.* **2006**, *128*, 16864.

(51) A. L. Benvin, Y. Creeger, G. W. Fisher, B. Ballou, A. S. Waggoner, B. A. Armitage, *J. Am. Chem. Soc.* **2007**, *129*, 2025.

(52) J. K. Hannestad, P. Sandin, B. Albinsson, *J. Am. Chem. Soc.*

2008, *130*, 15889.

(53) W. Su, M. Schuster, C. R. Bagshaw, U. Rant, G. A. Burley, *Angew. Chem. Int. Ed. Engl.* **2011**, *50*, 2712.

(54) D. Vasudevan, E. Y. Chua, C. A. Davey, *J. Mol. Biol.* **2010**, *403*, 1.

Figure Legends

Figure 1. (A) Structures of Py-Im polyamides **1** and **2**, Cy3-succinimidyl ester **3**, Cy5-succinimidyl ester **4**, and Cy3- or Cy5-conjugated Py-Im polyamide **5**-**8**. (B) Sequence of 5′-biotinylated hairpin DNA (ODN1 and ODN2). X represents biotin. The binding sequences of the Py-Im polyamides are shown in bold.

Figure 2. A schematic of construction of the pYT145-24 plasmid.

Figure 3. Preparation of the nucleosome. (A) The 145-bp DNA was prepared from pYT145-24. After digestion of pYT145-24 with *Eco*RV, the 145-bp DNA was purified as described in the Experimental Section. (B) A schematic of nucleosome preaparation. (C) Composition of the Nucleosome. After the preparation, the nucleosome was analyzed using 5 % polyacrylamide gel electrophoresis. Lane 1: the 145-bp DNA; lane 2: the nucleosome.

Figure 4. Structure of the mononucleosome and the Py-Im polyamide binding sites. (A) The ribbon model is the crystal structure of a Xenopus laevis nucleosome core particle (Protein Data Bank code 3LZ0).[54] The white arrow above the mononucleosome indicates a pseudo 2-fold axis passing through the center of the structure. The right panel displays an axial view of the mononucleosome. The target DNA sites for **1** and **2** are colored green and red, respectively. (B) DNA sequence of the 145-bp DNA fragment. The target DNA sites for **1** and **2** are colored green and red, respectively.

Figure 5. SPR sensorgrams for the interaction of Py-Im polyamides with hairpin DNAs immobilized on a sensor chip SA. (A) Py-Im polyamide **1** with ODN1 at a concentration ranging from 1.25×10^{-8} M (lowest curve) to 2.0×10^{-7} M (highest curve). (B) Py-Im polyamide **2** with ODN2 at a concentration ranging from 6.25×10^{-9} M (lowest curve) to 1.0×10^{-7} M (highest curve). (C) Py-Im polyamide **5** with ODN1 at a concentration ranging from 2.5×10^{-8} M (lowest curve) to 4.0×10^{-7} M (highest curve). (D) Py-Im polyamide **6** with ODN1 at a concentration ranging from 2.5×10^{-8} M

(lowest curve) to 4.0×10^{-7} M (highest curve). (E) Py-Im polyamide **7** with ODN2 at a concentration ranging from 2.5×10^{-8} M (lowest curve) to 4.0×10^{-7} M (highest curve). (F) Py-Im polyamide **8** with ODN2 at a concentration ranging from 2.5×10^{-8} M (lowest curve) to 4.0×10^{-7} M (highest curve).

Figure 6. Emission spectra of Cy3- or Cy5-conjugated Py-Im polyamides. The concentration of each Py-Im polyamide was 50 nM. (A) Emission spectra of **3**, **5** and **7**; λ_{ex} = 520 nm. (B) Emission spectra of **4**, **6** and **8**; λ_{ex} = 630 nm. (C) Emission spectra of **5** in the presence of its target DNA; λ_{ex} = 520 nm. (D) Emission spectra of **6** in the presence of its target DNA; λ_{ex} = 630 nm. (E) Emission spectra of **7** in the presence of its target DNA; λ_{ex}= 520 nm. (F) Emission spectra of **8** in the presence of its target DNA; λ_{ex}= 630 nm.

Figure 7. FRET between **5** and **8** on the same nucleosome. The concentration of each Py-Im polyamide, the 145-bp DNA and the nucleosome was 50 nM; λ_{ex} = 520 nm. (A) Emission spectra of **5** (blue) or **5** and **8** (red) in the presence of the-145 bp DNA. (B)

Emission spectra of **5** (blue) or **5** and **8** (red) in the presence of the nucleosome. (C) The calculated spillover from **5** in the mixture containing **5**, **8** and the nucleosome (blue) and emission spectrum of **5** and **8** in the presence of the nucleosome (red). (D) Fluorescence intensity of **8** was increased by **5** and the nucleosome. Emission spectra in the absence (blue) and presence (red) of the nucleosome, and the calculated emission spectrum of **8** in the mixture containing **5** and the nucleosome (green).

Figure 8. FRET between **7** and **6** on the same nucleosome. The concentration of each Py-Im polyamide, the 145-bp DNA and the nucleosome was 50 nM; λ_{ex} = 520 nm. (A) Emission spectra of **7** (blue) or **7** and **6** (red) in the presence of the 145-bp DNA. (B) Emission spectra of **7** (blue) or **7** and **6** (red) in the presence of the nucleosome. (C) The calculated spillover from **7** in the mixture containing **7**, **6**, and the nucleosome (blue) and the emission spectrum of **7** and **6** in the presence of the nucleosome (red). (D) Fluorescence intensity of **7** was increased by **6** and the nucleosome. Emission spectra of **7** in the absence (blue) and presence (red) of the nucleosome, and the calculated emission spectrum of **7** in the mixture containing **6** and the nucleosome (green).

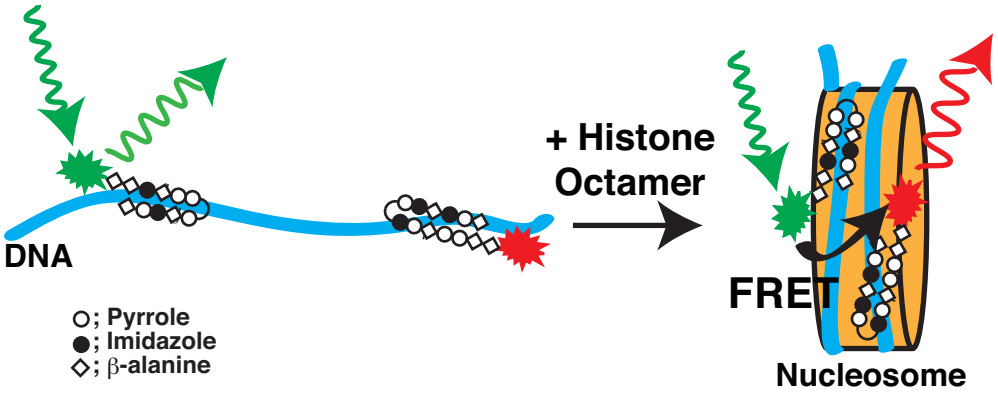

Graphical Abstract

(A)

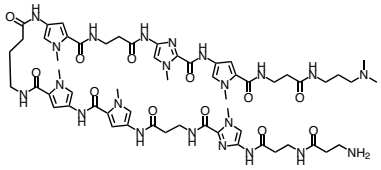

1: ββImβPyPyγPyβImPyβDp

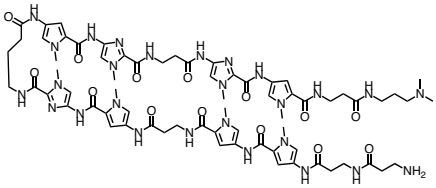

2: ββPyPyβPyImγPyImβImPyβDp

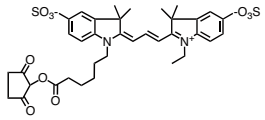

3: Cy3 *N*-hydroxysuccimide ester

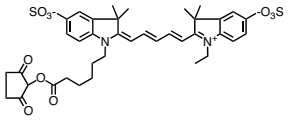

4: Cy5 *N*-hydroxysuccimide ester

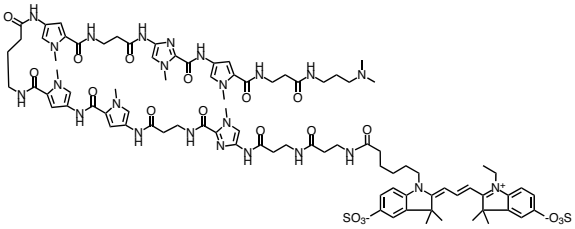

5: Cy3-ββImβPyPyγPyβImPyβDp

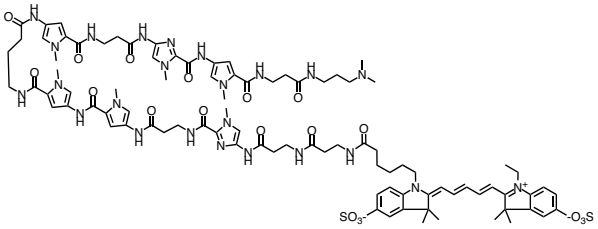

6: Cy5-ββImβPyPyγPyβImPyβDp

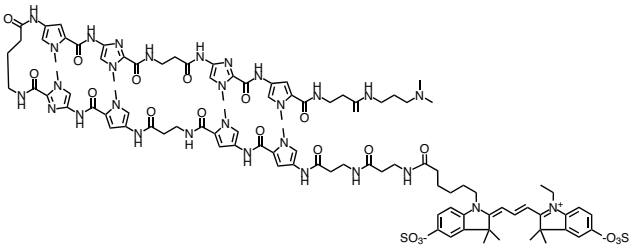

7: Cy3-ββPyPyβPyImγPyImβImPyβDp

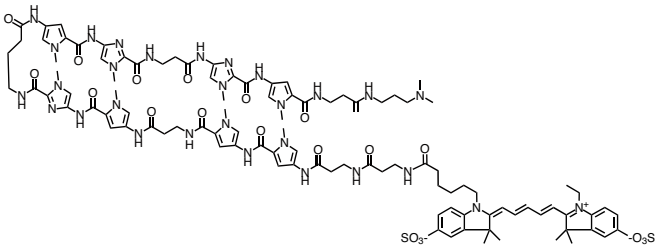

8: Cy5-ββPyPyβPyImγPyImβImPyβDp

(B)

ODN1 5′-XGCC**ATAGC**GGC$^{T}_{T}$
3′-CGG**TATCG**CCG$_{T}^{T}$

ODN2 5′-XGCC**ACGTGT**GGC$^{T}_{T}$
3′-CGG**TGCACA**CCG$_{T}^{T}$

Figure 1

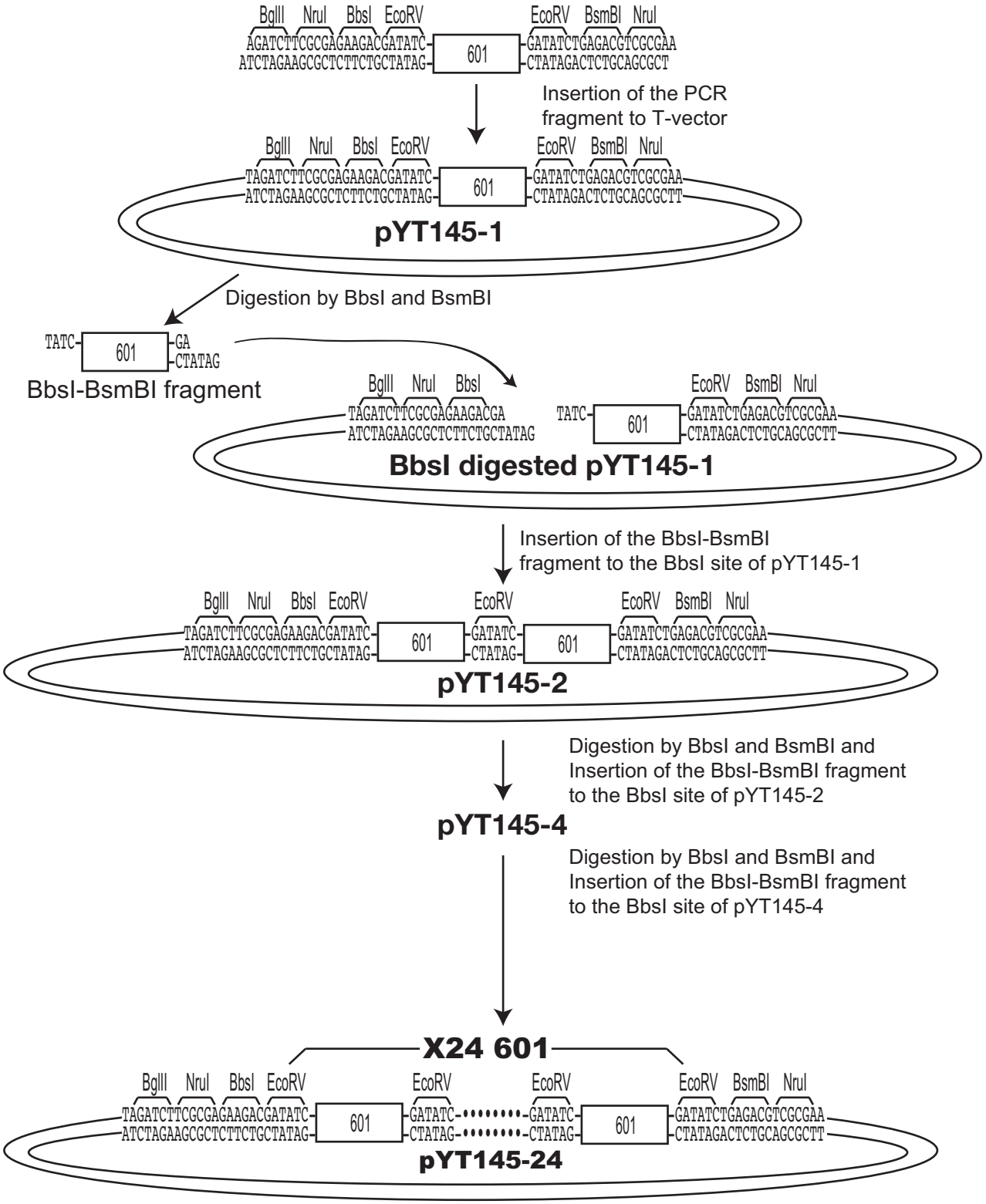

Multiple BbsI-BsmI fragments were coincidently inserted into the BbsI site of pYT145-4

Figure 2

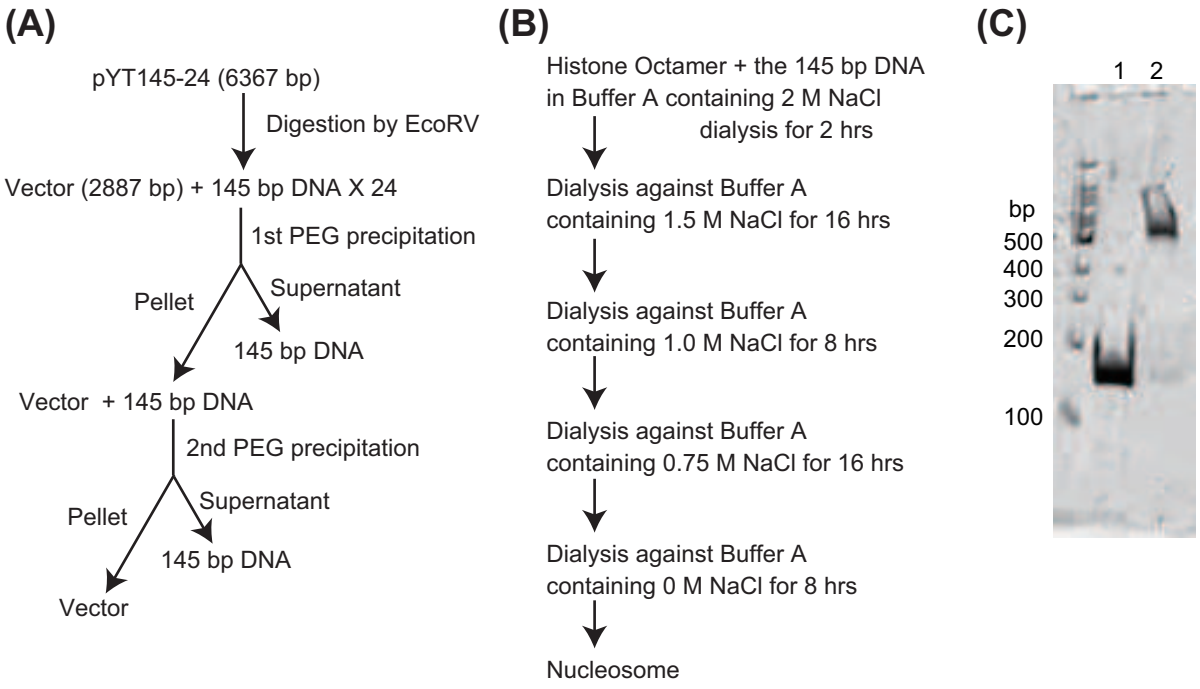
(A)
pYT145-24 (6367 bp)
Digestion by EcoRV
Vector (2887 bp) + 145 bp DNA X 24
1st PEG precipitation
Pellet
Supernatant
145 bp DNA
Vector + 145 bp DNA
2nd PEG precipitation
Pellet
Supernatant
145 bp DNA
Vector
(B)
Histone Octamer + the 145 bp DNA in Buffer A containing 2 M NaCl
dialysis for 2 hrs
Dialysis against Buffer A containing 1.5 M NaCl for 16 hrs
Dialysis against Buffer A containing 1.0 M NaCl for 8 hrs
Dialysis against Buffer A containing 0.75 M NaCl for 16 hrs
Dialysis against Buffer A containing 0 M NaCl for 8 hrs
Nucleosome
(C)
1 2
bp
500
400
300
200
100

Figure 3

(A)

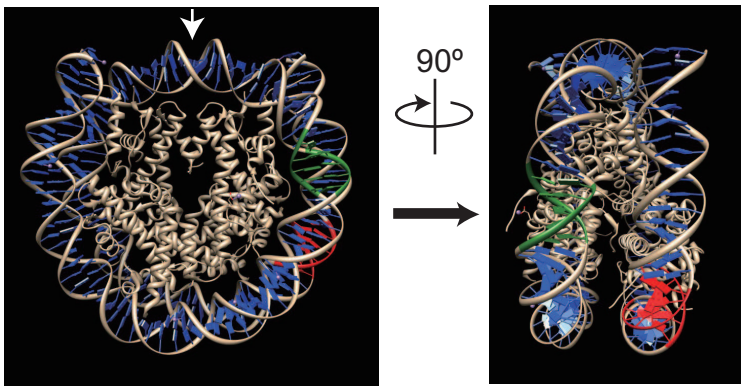

(B)

```
5′ ATCAGAATCC CGGTGCCGAG GCCGCTCAAT
3′ TAGTCTTAGG GCCACGGCTC CGGCGAGTTA

   TGGTCGTAGA CAGCTCTAGC ACCGCTTAAA
   ACCAGCATCT GTCGAGATCG TGGCGAATTT

   CGCACGTACG CGCTGTCCCC CGCGTTTTAA
   GCGTGCATGC GCGACAGGGG GCGCAAAATT

   CCGCCAAGGG GATTACTCCC TAGTCTCCAG
   GGCGGTTCCC CTAATGAGGG ATCAGAGGTC

   GCACGTGTCA GATATATACA TCGAT 3′
   CGTGCACAGT CTATATATGT AGCTA 5′
```

Figure 4

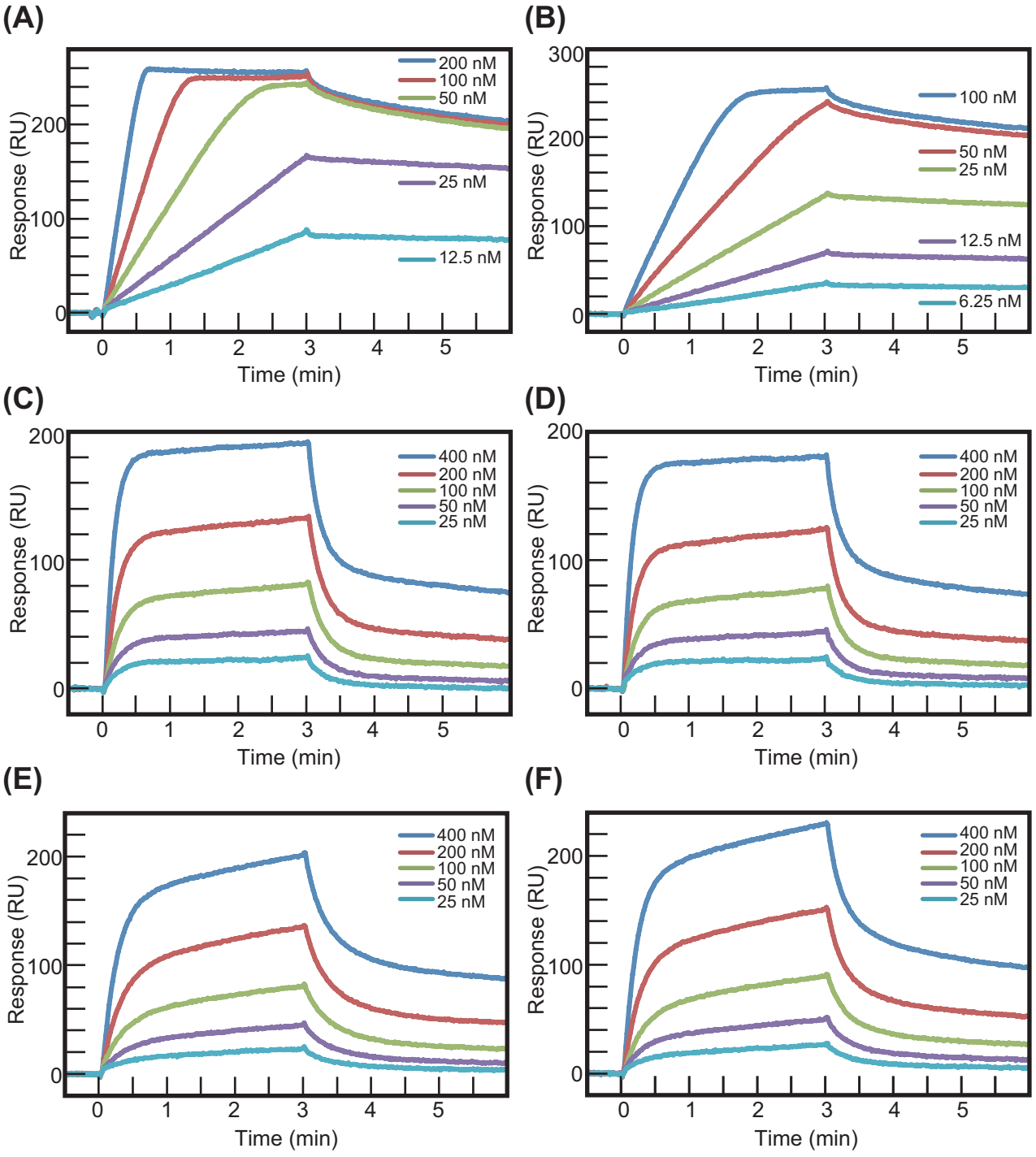
(A)
Response (RU)
Time (min)
200 nM
100 nM
50 nM
25 nM
12.5 nM
(B)
Response (RU)
Time (min)
100 nM
50 nM
25 nM
12.5 nM
6.25 nM
(C)
Response (RU)
Time (min)
400 nM
200 nM
100 nM
50 nM
25 nM
(D)
Response (RU)
Time (min)
400 nM
200 nM
100 nM
50 nM
25 nM
(E)
Response (RU)
Time (min)
400 nM
200 nM
100 nM
50 nM
25 nM
(F)
Response (RU)
Time (min)
400 nM
200 nM
100 nM
50 nM
25 nM

Figure 5

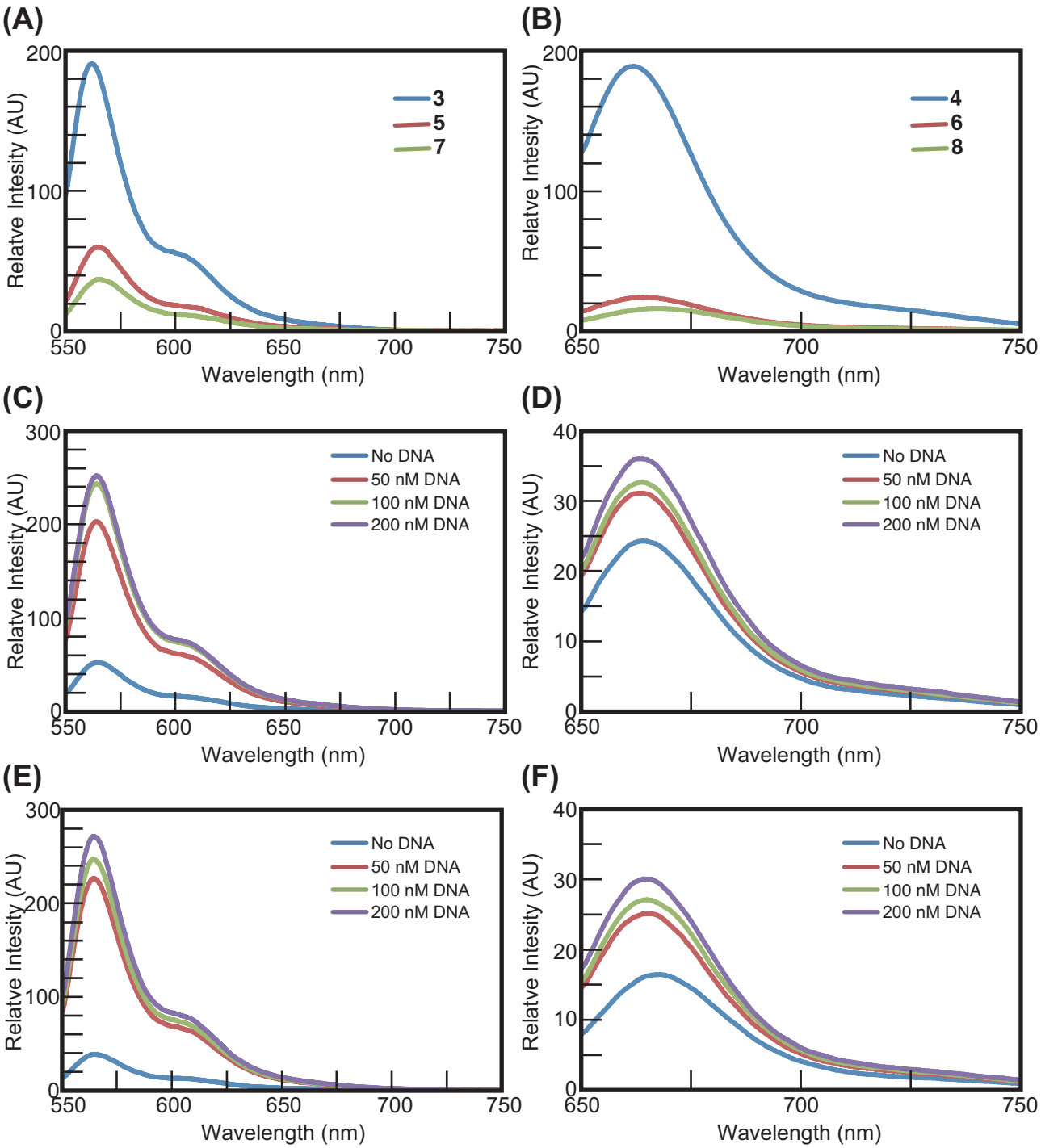
(A)
Relative Intesity (AU)
Wavelength (nm)
3
5
7
(B)
Relative Intesity (AU)
Wavelength (nm)
4
6
8
(C)
Relatve Intesity (AU)
Wavelength (nm)
No DNA
50 nM DNA
100 nM DNA
200 nM DNA
(D)
Relative Intesity (AU)
Wavelength (nm)
No DNA
50 nM DNA
100 nM DNA
200 nM DNA
(E)
Relatve Intesity (AU)
Wavelength (nm)
No DNA
50 nM DNA
100 nM DNA
200 nM DNA
(F)
Relative Intesity (AU)
Wavelength (nm)
No DNA
50 nM DNA
100 nM DNA
200 nM DNA

Figure 6

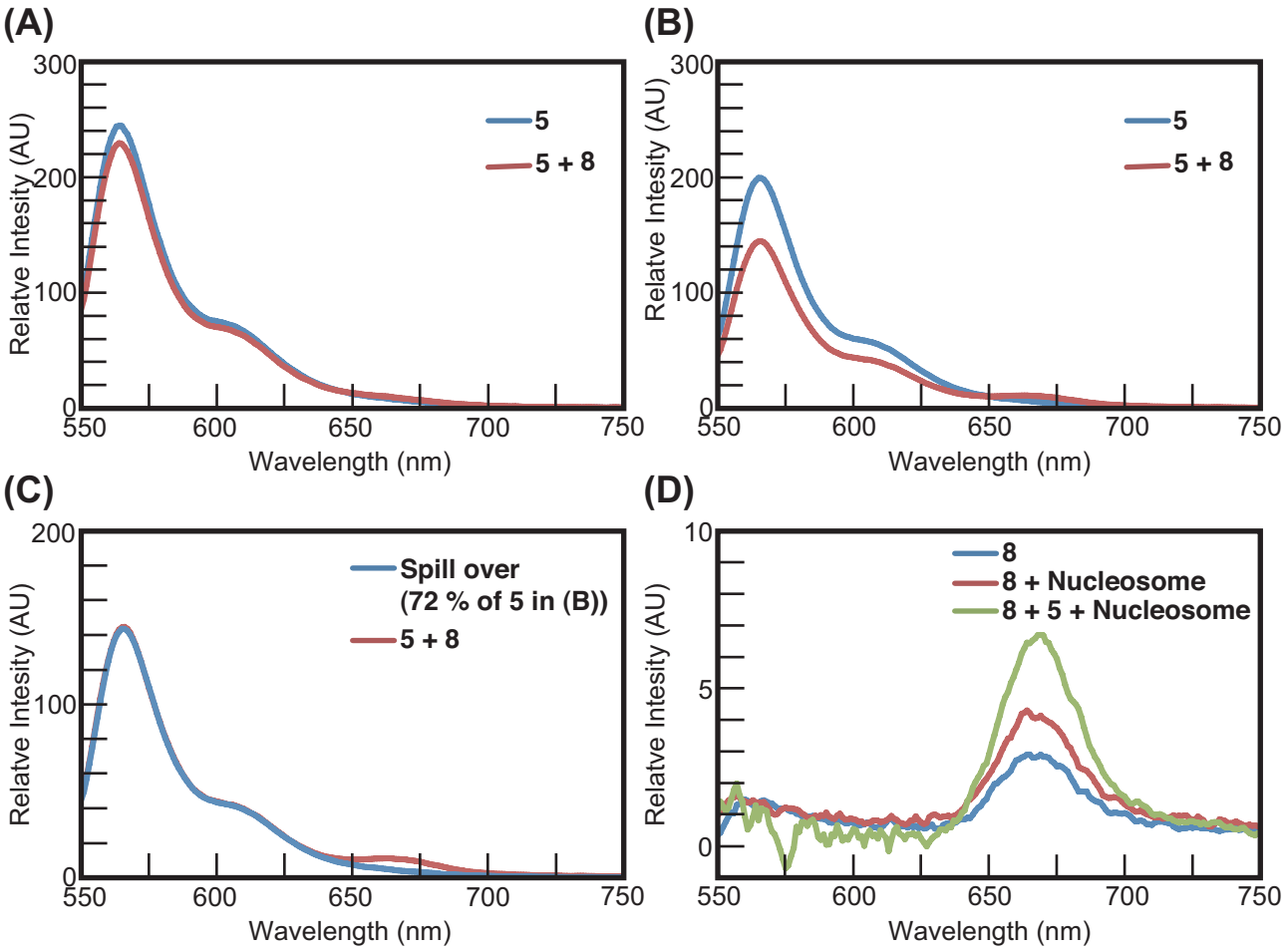
(A)
Relative Intesity (AU)
300
200
100
0
550
600
650
700
750
Wavelength (nm)
5
5 + 8
(B)
Relative Intesity (AU)
300
200
100
0
550
600
650
700
750
Wavelength (nm)
5
5 + 8
(C)
Relative Intesity (AU)
200
100
0
550
600
650
700
750
Wavelength (nm)
Spill over
(72 % of 5 in (B))
5 + 8
(D)
Relative Intesity (AU)
10
5
0
550
600
650
700
750
Wavelength (nm)
8
8 + Nucleosome
8 + 5 + Nucleosome

Figure 7

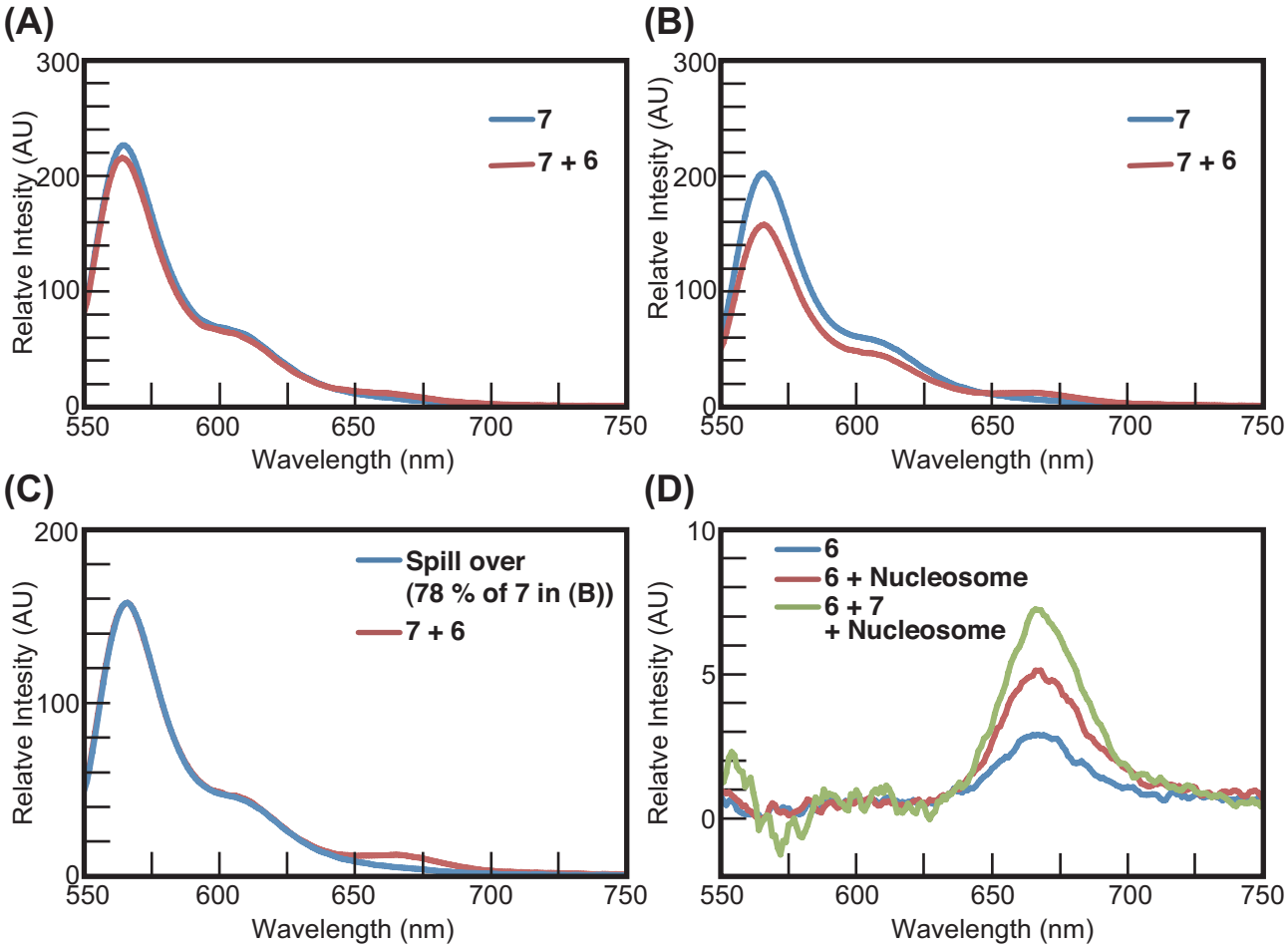
(A)
Relative Intesity (AU)
300
200
100
0
550
600
650
700
750
Wavelength (nm)
7
7 + 6
(B)
Relative Intesity (AU)
300
200
100
0
550
600
650
700
750
Wavelength (nm)
7
7 + 6
(C)
Relative Intesity (AU)
200
100
0
550
600
650
700
750
Wavelength (nm)
Spill over
(78 % of 7 in (B))
7 + 6
(D)
Relative Intesity (AU)
10
5
0
550
600
650
700
750
Wavelength (nm)
6
6 + Nucleosome
6 + 7
+ Nucleosome

Figure 8

Table 1 Binding affinity of **1**, **2** and, **5**-**8** with the respective target DNAs

Py-Im polyamide[a]	K_D (10^{-7} M)	k_a (10^4 $M^{-1}s^{-1}$)	k_d (10^{-3} s^{-1})
1 	0.010 ± 0.0012	830 ± 410	8.7 ± 3.9
2 	0.0059 ± 0.0037	290 ± 130	1.7 ± 1.4
5 	3.5 ± 0.88	11 ± 3.7	38 ± 6.2
6 	0.64 ± 0.50	59 ± 44	38 ± 19
7 	3.1 ± 0.71	6.4 ± 0.13	20 ± 5.0
8 	5.1 ± 0.32	5.5 ± 0.94	28 ± 3.9

[a]Closed circle, Open circle, and β indicate Im, Py, and β-alanine, respectively.